

Are micelles actually at the interface in micellar casein stabilized foam and emulsions?

Xilong Zhou^a, Jack Yang^b, Guido Sala^a, Leonard M.C. Sagis^{a,*}

^a Physics and Physical Chemistry of Foods, Wageningen University, Bornse Weilanden 9, 6708WG, Wageningen, the Netherlands

^b Biobased Chemistry & Technology, Wageningen University, Bornse Weilanden 9, 6708WG, Wageningen, the Netherlands

ARTICLE INFO

Keywords:

Casein micelles
Small casein aggregates
 β -Casein
Interfacial rheology
Interfaces

ABSTRACT

Different casein preparations are used for stabilizing emulsions and foams. For systems made with aqueous micellar casein dispersions, the molecular and colloidal mechanisms responsible for the stabilization of oil-water and air-water interfaces have not been conclusively ascertained. Whether the micelles themselves, small casein aggregates, or individual casein molecules are at the interface is still an open question. Understanding these mechanisms is important for food industries to improve product formulations. We investigated the nonlinear rheology and microstructure of oil-water and air-water interfaces stabilized with casein micelle dispersions and their fractions. Our results convincingly show that the micelles themselves are not adsorbed at the interfaces. For air-water interfaces, the behavior appears to be dominated by β -casein, whereas the properties of oil-water interfaces are dominated by small casein aggregates. These findings are important to understand the stabilization mechanisms of emulsions and foams prepared with caseins or milk.

1. Introduction

Dairy proteins are widely used as stabilizers in food emulsions and foams (Scott, Duncan, Sumner, & Waterman, 2003; Tomas, Paquet, Courthaudon, & Lorient, 1994; Wu et al., 2016; Zhou et al., 2016). Huppertz (2010) and Ho, Bhandari, and Bansal (2021) comprehensively reviewed the influence of milk protein composition and different processing parameters on milk protein stabilized foams. A detailed review of emulsifying and emulsion stabilizing properties of milk proteins can be found in Dickinson's review papers (Dickinson, 1997, 2001). There is a consensus that dairy proteins form viscoelastic interfacial layers at air-water or oil-water interfaces, providing steric and electrostatic repulsion, thus stabilizing emulsion droplets or foam bubbles against coalescence. The rheological properties of interfaces stabilized with α_{S1} -, β -casein or β -lactoglobulin are extensively studied in the small deformation regime (Dickinson, 1998). However, the interfacial rheology of oil-water or air-water interfaces in the nonlinear regime is hardly reported, in spite of its high relevance for processing and consumption (Sagis & Fischer, 2014). In previous studies on the microstructure and dilatational properties of whey proteins at the oil-water (Zhou, Sala, & Sagis, 2020) and air-water interfaces (Yang, Thielen, Berton-Carabin, van der Linden, & Sagis, 2020), we showed that native whey proteins

form viscoelastic solid-like interfaces, which have a yield stress. Beyond this yield stress the interface shows significant softening and behaves more like a viscoelastic fluid. For the other major constituent of dairy protein, casein, more research is needed to establish its behavior in the nonlinear regime.

Casein is regarded as a good emulsifier that can reduce the surface tension to a great extent (Jackson & Pallansch, 1961; Leman, Kinsella, & Kilara, 1989). It is mainly composed of four types of monomers, κ -casein, α_{S2} -casein, α_{S1} -casein, and β -casein, with a ratio 1.3 : 1 : 4 : 4 (Walstra, 1990). These monomers form micelles, where they are linked to each other by hydrophobic interactions and hydrogen bonds, and by colloidal calcium phosphates. Over 95% of the casein in milk is present in the casein micelles (Dumpler, 2017). In the past decades, most research investigating the role of casein in emulsions, foams, or interfaces in general, were mostly based on sodium caseinate, and to a lesser extent on micellar casein. It has been shown that casein exhibits different hydrophobicity and surfactant properties depending on its structural aggregation state (Courthaudon et al., 1999; Roman & Sgarbieri, 2006). The results obtained for sodium caseinate cannot be extrapolated to micellar caseins, as the micelles are broken down during the manufacturing of sodium caseinates (Carr & Golding, 2016). Only a few studies cast light on the application of casein micelles in emulsions

* Corresponding author.

E-mail address: leonard.sagis@wur.nl (L.M.C. Sagis).

<https://doi.org/10.1016/j.foodhyd.2022.107610>

Received 23 September 2021; Received in revised form 18 February 2022; Accepted 21 February 2022

Available online 26 February 2022

0268-005X/© 2022 The Authors. Published by Elsevier Ltd. This is an open access article under the CC BY license (<http://creativecommons.org/licenses/by/4.0/>).

and foams. Lazzaro et al. (2017) disaggregated casein micelles into different sizes by gradually demineralizing casein micelles, and found monomers or smaller casein micelles have better emulsifying properties, but are less stable to creaming and flocculation. Zhang and Goff (2004) utilized EDTA to disaggregate casein micelles in milk protein solution and achieved better foamability. Some other studies investigated the effects of pH, ionic strength (Zhang, Dalgleish, & Goff, 2004), and heat treatment (Liang, Patel, Matia-Merino, Ye, & Golding, 2013) on the stability of emulsions or foams stabilized by casein micelles or by full milk proteins. A common observation of these studies is that nonmicellar caseins always display a better emulsifying property or formability than micellar casein. Although the foamability of casein micelles is not comparable with nonmicellar caseins, micellar casein appears to provide better foam stability. Li et al. (2020) applied casein micelles in recombinant dairy cream and achieved better foam stability after whipping. Ewert et al. (2016) also proved that comparing with sodium caseinate, micellar caseins produced a more stable foam. Casein micelles (Dombrowski, Dechau, & Kulozik, 2016) or casein micelle aggregates (Chen et al., 2016) have larger molecular size and likely to retard the drainage of liquid from the films separating the bubbles, thus improving the stability of foams. However, the molecular and colloidal mechanisms behind the stabilization of oil-water (O-W) and air-water (A-W) interfaces by micellar casein, are still under debate, and published studies even contradict each other.

For foams, casein micelles (Dombrowski et al., 2016) and casein micelle aggregates (Chen et al., 2016) appeared not to adsorb at the interface, and were assumed to either remain in the bulk phase, or attach to the interface as a sublayer, leading to pinning of the foam lamellae and slowing down drainage (Chen et al., 2017). However, this behavior has not been fully proved, and contradictory findings were reported in other research (Silva, Saint-Jalmes, de Carvalho, & Gaucheron, 2014), where casein micelles are claimed to adsorb at the A-W interface and subsequently fall apart. Regarding emulsions, some researchers stated that casein micelles can adsorb at the O-W interface (San Martín-González, Roach, & Harte, 2009) and stabilize the emulsions by the so-called Pickering mechanism (Dickinson, 2015). Although electron microscopy pictures do illustrate that micelles can be at oil-water or air-water interfaces (Anderson, Brooker, & Needs, 1987; Brooker, 1985; Jensen, 2013), it is difficult to distinguish whether in these cases the micelles adsorbed at the interfaces or just attached to the interface as a sublayer. Moreover, in those pictures, only a few complete micelles could be found at the interfaces. Whether those sparse micelles at the interfaces can stabilize the droplets or foams is questionable. So, whether micellar casein can adsorb at O-W interfaces and thus prevent oil droplet coalescence is also not completely clear yet.

In this study, a casein micelle dispersion was fractionated by ultracentrifugation into a pellet (which was subsequently redispersed in water), and a supernatant. The pellet redispersion was mainly composed of micellar caseins, and the supernatant contained small aggregates and monomers of all casein fractions. We investigated the nonlinear rheology of O-W and A-W interfaces stabilized with the casein micelle dispersion and the other two fractions separately. We analyzed the interfaces using multiphoton excitation microscopy (MPM) and ellipsometry. The microstructure of A-W interfaces was also visualized by atomic force microscopy on Langmuir-Blodgett films. We aimed at explaining how casein micelles stabilize O-W and A-W interfaces on the basis of molecular and colloidal mechanisms.

2. Methods

2.1. Materials

Micellar casein isolate (84.15% protein, lactose 3.0%, ash 7.3%, moisture 3.3%, fat 1.1%) was kindly donated by FrieslandCampina (Netherlands). Beta-casein powder (79.33% protein) was purchased from Eurial (France). Florisil (60–100 mesh), dimethyl sulfoxide

(DMSO), syringe filters (PVDF, 5.0 μm , d 25 mm; PVDF, 0.45 μm , d 33 mm; PVDF, 0.1 μm , d 33 mm) and filter membrane (PVDF, 0.45 μm , d 47 mm) were purchased from Merck (Netherlands). Medium chain triglyceride (MCT) was purchased from IMCD (France). Cyanine 5 (Cy5) was purchased from Lumiprobe (Europe). UV glue, nylon rings (M10) and metal washers (diameter 7 mm) were purchased online (Amazon). Glass slides (#1.5) were purchased from Thermo (Netherlands). Dialysis membranes (3.5 kD, #3) were purchased from Spectrum Labs (Greece).

2.2. Fractionation of casein micelle dispersion

A casein micelle dispersion with 2.0 wt% protein was made by dissolving micellar casein isolate in Milli-Q water and stirring overnight at room temperature; 0.02 wt% sodium azide was added to prevent spoilage. The casein micelle dispersion was filtered through syringe filters with a cut off 5.0 μm and 0.45 μm , successively.

Twenty gram of casein micelle dispersion was centrifuged at 15,000 g for 1 h using an ultracentrifuge (Beckman Coulter, US). The supernatant was carefully transferred to a serum bottle with a volume of 20 mL, and the mass was compensated to 20 g by adding Milli-Q water. The supernatant was subsequently filtered using a syringe filter with a cut off 0.1 μm .

After the first ultracentrifugation, the pellet still contained a significant amount of liquid. To get rid of the monomers and small aggregates in that fluid, the pellet was washed. First, Milli-Q water was added to the tube to achieve a total mass of 20 g. Then the pellet was re-dispersed using a Turrax (IKA T25, Germany) at 8000 rpm. Subsequently, the dispersion was ultracentrifuged at 50,000 g for 30 min. The new supernatant was discarded, and the new pellet was washed again. After two full washing steps, the final pellet was re-dispersed, and sonicated for 10 min (160 W, 35 kHz) using an ultrasonic bath (RK510, Bandelin, Germany), then filtered through syringe filters with a cutoff of 5.0 μm and 0.45 μm , successively.

The protein concentration of the casein micelle dispersion, supernatant and pellet redispersion was determined by DUMAS with conversion coefficient 6.38, and the contents were 1.90 ± 0.06 , 0.31 ± 0.02 , and 1.26 ± 0.01 wt%, respectively.

2.3. Particle size distribution of the samples

The particle size distribution of casein micelle dispersion, supernatant and pellet were determined using a Malvern Zetasizer Nano-ZS (Malvern Instruments Ltd, United Kingdom). All samples were diluted to a protein concentration 0.1 wt% with Milli-Q water. Approximately 1 mL sample was pipetted into a cuvette (type DTS0012). The refractive index and absorption indices of protein dispersions/solutions were 1.450 and 0.001, respectively. The refractive index of dispersant (water) was 1.330. Before each test, the sample was equilibrated for 2 min.

2.4. Fat purification

The anhydrous milk fat (AMF) used for the study of the rheological properties of O-W interfaces prepared with the different protein samples and for the other analyses described here below, was previously purified. Florisil was desiccated overnight at 105 °C in an oven, then cooled down to room temperature. AMF was melted at 60 °C and mixed with 10 wt% Florisil. The mixture was stirred at 60 °C for at least 2 h. Subsequently, 10 mL of the mixture was sampled and filtered with a syringe filter to remove Florisil particles. The surface tension of the interface between the filtered AMF and Milli-Q water was tested for at least 1 h. If the tension decreased over time, AMF needed to be purified further by repeating the steps described above. Once the surface tension stayed constant, the AMF and Florisil mixture were filtered using vacuum filtration with a filter membrane (PVDF, 0.45 μm , d 47 mm). The filtered AMF was sealed in blue cap bottles and kept in the dark at room temperature.

The medium chain triglyceride oil (MCT) for the microscopy tests was also purified according to the same protocol, but at room temperature.

2.5. Oscillatory dilatational measurements

Oscillatory dilatational deformations were applied to the O–W or A–W interfaces using a Tracker Automated Droplet Tensiometer (Teclis, France) according to the method described by Zhou et al. (2020). For O–W interfaces, purified AMF was transferred to the cuvette and kept melted at 40 °C in the cell. A pendent droplet of the protein samples was formed at the tip of the needle, which was immersed in the oil phase. The surface area of the droplet was 20 mm². The density of the droplet fluid and AMF at 40 °C were 0.9922 and 0.9041 g/mL, respectively. For the A–W interface, a pendent droplet of protein solution was formed at the tip of the needle at 20 °C. A small amount of water was added at the bottom of cuvette to saturate the air phase with water and limit evaporation during the test. For that same purpose, the cuvette was covered with parafilm. The area of the droplet was adjusted to 15 mm². The density of the droplet fluid and air at 20 °C were 0.9982 and 0.0012 g/mL, respectively.

The interface was firstly equilibrated for 3 h, followed by sinusoidal area deformations. An amplitude sweep was performed with amplitudes of 5, 10, 15, 20 and 30%, at a fixed frequency of 0.01 Hz. For every amplitude, 5 oscillation cycles were performed and followed by a 900 s of rest. For every amplitude, only the middle 3 cycles were used to construct Lissajous plots, where surface pressure (Π) is plotted against strain amplitude (γ). The method of constructing Lissajous plots was introduced by Sagis and Fischer (2014). The surface pressure and deformation were calculated using:

$$\gamma = \frac{A_t - A_0}{A_0} \quad 2$$

$$\pi = \sigma_t - \sigma_0 \quad 3$$

where A_t and σ_t are interfacial area and interfacial tension at time t ; A_0 and σ_0 are initial interfacial area and interfacial tension.

2.6. Visualization of interfaces with multiphoton excitation microscopy (MPM)

2.6.1. Object slides for MPM

Pictures of the object slides used for MPM are shown in Fig. 1a. A metal washer and a nylon ring were attached on a glass slide using liquid

UV glue, then the whole setup was incubated with UV light overnight to solidify the glue.

2.6.2. Protein dialysis

Cyanine 5 was dissolved in dimethyl sulfoxide (DMSO) to a concentration of 1 mg/mL. Then, 10 and 50 μ L Cyanine 5 solution were added to 1 mL supernatant solution and pellet redispersion, respectively. The corresponding blank samples were made by adding the same amount of dye to 1 mL Milli-Q water. The samples were incubated in the dark for 2 h at room temperature. Subsequently, the samples were dialyzed with a cutoff size of 3.5 kDa for 7 h by flowing Milli-Q water at room temperature.

2.6.3. Visualization of the interfaces

The dialyzed sample was slowly pipetted into cell 1 (Fig. 1a), until the sample formed a meniscus. For O–W interfaces, the outside of the meniscus was covered with MCT oil (Fig. 1c). For A–W interfaces, the slide was covered by parafilm to prevent evaporation. A small amount of water was added in cell 2 to limit sample evaporation (Fig. 1b). O–W and A–W interfaces were visualized by a Leica SP8Dive multiphoton excitation microscope (Leica, Germany), using a HC FLUOTAR L 25 \times /0.95 W VISIR objective. The laser excitation wavelength was set at 840 nm, and the emission range for the detector was 650–700 nm. A 3-dimensional region (240 \times 240 \times 200 μ m) was scanned by the MPM.

2.7. Topography of interfacial microstructure

2.7.1. Interfacial pressure isotherms

Interfacial pressure isotherms (area vs. surface pressure) were made using a Langmuir trough (KSV NIMA/Biolin Scientific Oy, Finland). Casein micelle dispersion, supernatant, and pellet redispersion were diluted to 0.2 wt%. The samples were injected (200 μ L) at the bottom of a Langmuir trough filled with Milli-Q water using a gas-tight syringe. Afterwards, the system was equilibrated for 3 h, while monitoring the surface pressure using a platinum Wilhelmy plate (perimeter 20 mm, height 10 mm). At last, the interfacial area was reduced by compressing the film with Teflon barriers, moving with a speed of 5 mm/min.

2.7.2. Preparation of Langmuir-Blodgett (LB) films

LB films were made based on the same protocol described for the interfacial pressure isotherms. A freshly cleaved mica sheet (Highest Grade V1 Mica, Ted Pella, USA) was fixed vertically with respect to the interface. The mica sheet was completely immersed in the water phase. An amount of 200 μ L of sample was injected at the bottom of the trough,

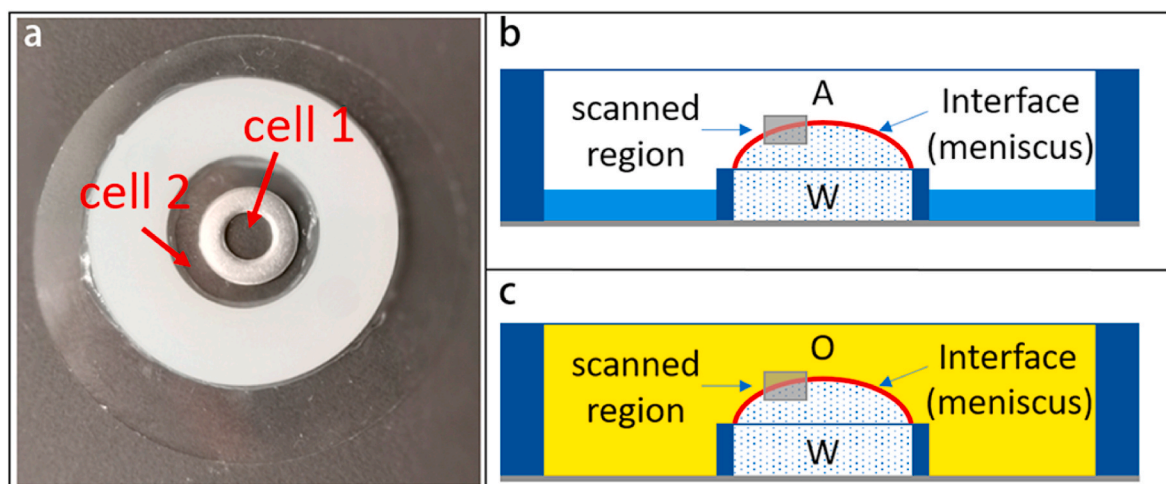


Fig. 1. Picture and schematics of slides for MPM. (a) top view of the slide; (b) side view of the slide for the A–W interface; (c) side view of the slide for the O–W interface. ‘A’ represents air; ‘W’ represents the water phase with proteins; ‘O’ represents oil.

while monitoring the surface pressure using a platinum Wilhelmy plate. After equilibrating for 3 h, the films formed at the interface were compressed to a target surface pressure of 13 or 23 mN/m. The interfacial films were deposited on the sheet mica by withdrawing the sheet vertically at a speed of 1 mm/min, while the Teflon barriers maintained the target surface pressure. All films were produced in duplicate and dried for two days in a desiccator at room temperature.

2.7.3. Atomic force microscopy (AFM)

The topography of the LB-films was studied using AFM (MultiMode 8-HR, Bruker, USA). The films were analyzed in tapping mode with a ScanAsyst-air model non-conductive pyramidal silicon nitride probe (Bruker, USA). A normal spring constant of 0.40 N/m and a lateral scan frequency of 0.977 Hz were applied for the analysis. The films were scanned for a $2.0 \times 2.0 \mu\text{m}^2$ area with a lateral resolution of 512×512 pixels². To ensure good representativeness, at least two locations of each replicate were scanned. The images were analyzed with Nanoscope Analysis v1.5 software (Bruker, USA).

2.7.4. Ellipsometry

The thickness of A-W and O-W interfacial films prepared with casein micelle dispersion, supernatant or redispersed pellet were analyzed with an imaging nulling ellipsometer EP4 (Accurion, Germany). A-W interfacial films were created by injecting 10 mL of protein solutions in Petri dishes. Afterwards, the measurement spot was aligned on the interfacial layer. For evaluation of the O-W interfaces, the light source and objective lens coupled to the analyzer were extended with light guides. O-W interfacial films were created in a Teflon trough by first injecting 15 mL protein solutions, followed by the alignment of measurement spot. The MCT oil was then carefully pipetted onto the top of the protein solution until the guides were immersed in the oil. Both A-W and O-W interfaces were equilibrated for 3 h. Afterwards, the interfacial films were measured over wavelength ranges varying from 499.8 to 793.8 nm of two zones at an angle of incidence of 50° to obtain the ellipsometric parameters phase shift (δ) and amplitude ratio (ψ). The measurements were performed at room temperature, and at least two independently prepared interfacial films were measured. A wavelength scan was also performed on Milli-Q-air and MCT-air interfaces to determine their refractive indices for the model fitting. The output of the protein layers was analyzed with the EPModel v3.6.1. Software provided by the supplier. A three layers system was built in the model by combining the air/oil layer, the protein layer, and the Milli-Q layer. The parameters of the protein layer in the model were fitted using a Cauchy model:

$$n(\lambda) = A + \frac{B}{\lambda^2} + \frac{C}{\lambda^4} \quad (4)$$

Where n is the refractive index; λ is the wavelength of the polarized light; A , B , and C are fitting parameters.

2.8. Statistical treatment of the data

All samples were prepared in duplicate, and all tests were performed at least twice. The data in this paper are reported as mean \pm standard deviation.

3. Results

3.1. Size distribution of different fractions of casein micelle dispersion

In order to compare the behavior of its different colloidal components at O-W and A-W interfaces, the casein dispersion was ultracentrifuged into two fractions, pellet and supernatant. The efficiency of separation was evaluated by testing the particle size distribution of casein micelle dispersion, pellet redispersion, and supernatant (Fig. 2). The size distributions of the pellet redispersion and casein micelle

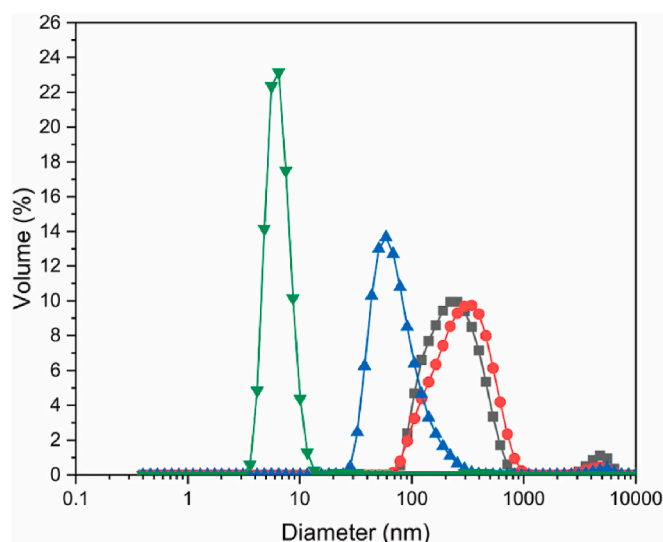


Fig. 2. Particle size distribution of the casein micelle dispersion (●), pellet redispersion (■), supernatant (▲) and β -casein solution (▼).

dispersion almost overlapped and presented a main peak at 200–400 nm, which is the typical size of casein micelles (Dalglish, Spagnuolo, & Goff, 2004; Fox & McSweeney, 2013; Walstra, 1990). The main peak of the curve of the supernatant was at 40–50 nm, i.e. a fraction which in older literature is often referred to as “submicelles” (Qi, 2007; Walstra, 1999). Here, we will refer to this fraction as “small aggregates”. The particle size distribution of a β -casein solution was analyzed, and showed a main peak around 6 nm. So, we can assume β -casein was mainly present in the solution in monomeric form. Basically, the results clearly show that the pellet redispersion was mainly composed of micellar caseins. The supernatant appeared to consist mainly of small aggregates, but contained undoubtedly also monomers of the various casein fractions. Casein micelles and other serum casein species, i.e., small aggregates or monomers are well known to coexist in dynamic equilibria, which are affected by pH, temperature, phosphate and ionic strength of Ca^{2+} (Schiffer, Scheidler, Kiefer, & Kulozik, 2021; Walstra, Wouters, & Geurts, 2005). The monomers could not be detected by the NanoSizer since the scattering was dominated by the small aggregates present in the samples. Compared with the monomer α -casein, β -casein is less charged and has more distinct hydrophobic and hydrophilic regions. As a result, it behaves like a low molecular weight surfactant (Dalglish & Leaver, 1991; Dickinson & Matsumura, 1994), and is more likely to adsorb at interfaces. It was even shown to displace α -casein from the interface, and also was dominant at the air-water interface when mixed with β -lactoglobulin (Mackie, Gunning, Ridout, Wilde, & Morris, 2001; Ridout, Mackie, & Wilde, 2004). Consequently, 0.2 wt% β -casein was used to investigate the role of monomers at the O-W and A-W interfaces.

3.2. Nonlinear rheology of O-W interfaces

A dilatational amplitude sweep at a frequency of 0.01 Hz was applied for interfaces stabilized with casein dispersion, supernatant or pellet redispersion, to ascertain which fraction of the solution dominated the response. Also, a β -casein solution was analyzed. The Lissajous plots of the O-W interfaces are shown in Fig. 3. At an amplitude of 10%, the response of the O-W interfaces stabilized with the casein dispersion was asymmetrical, which meant that at this strain amplitude the response was already in the nonlinear regime. The interfaces showed softening in expansion and hardening in compression. Softening was evidenced by the combination of a rapid increase of surface pressure at the beginning of the expansion (the upper part of the curve from left to right) followed

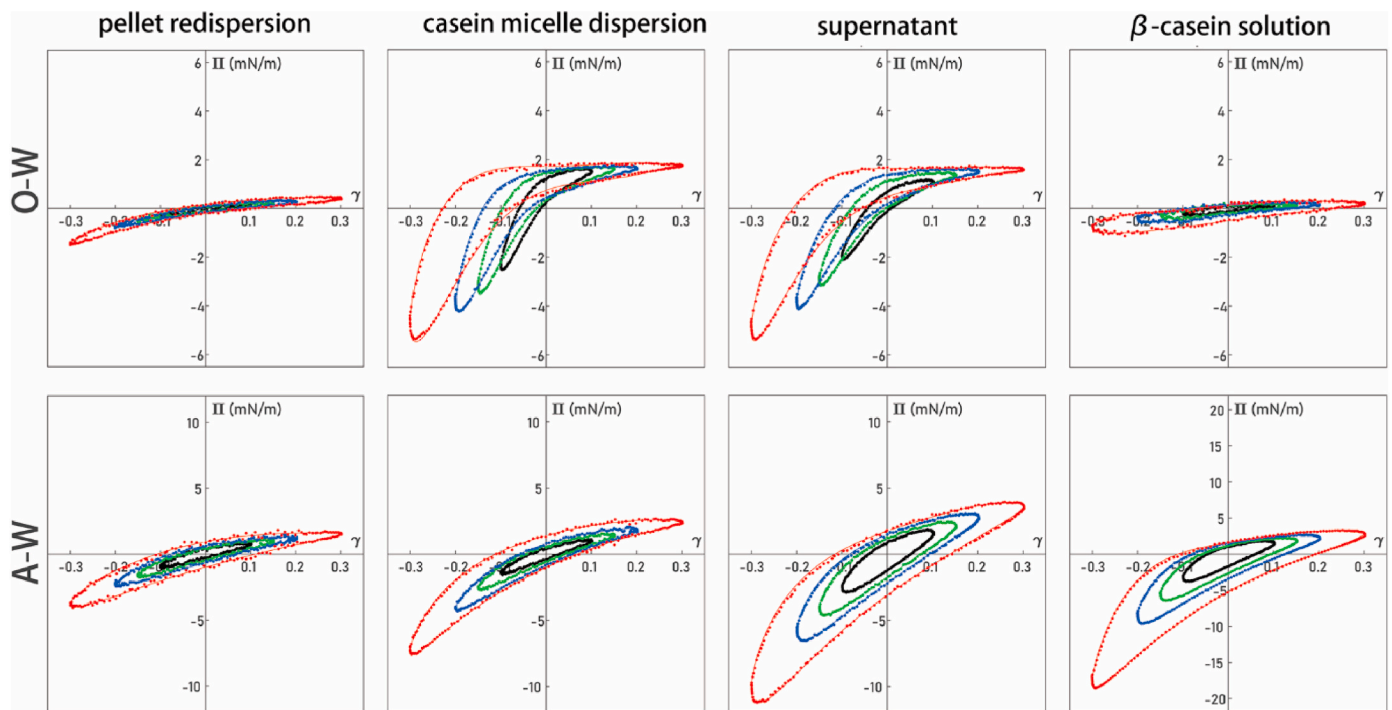


Fig. 3. Lissajous plots showing the surface pressure versus deformation for O–W and A–W interfaces stabilized with casein micelles dispersion, supernatant, pellet redispersion, or β -casein. The strain amplitudes were 10% (black), 15% (green), 20% (blue), 30% (red). The frequency was 0.01 Hz. (For interpretation of the references to color in this figure legend, the reader is referred to the Web version of this article.)

by a decrease in the slope of the curve towards the end of the expansion phase. Hardening was indicated by an increasing slope of the curve in compression (the bottom part of the curve from right to left). With an increase of the amplitude, the gradual softening behavior in expansion turned into yielding, as the slope of the surface pressure abruptly changed during expansion and reached a plateau where the slope of the curve was close to zero. Yielding and hardening behavior imply changes of the microstructure formed by the proteins at the interfaces. At the start of expansion, this structure was strong enough to resist the deformation and showed a highly stiff response. When the interfaces kept expanding, the structure was disrupted, leading to a significant decrease in stiffness, and a relatively more viscous response. In compression, the disrupted structure was densified, until the proteins reached a jammed (or gelled) state, which resulted in much stronger molecular interactions and an abrupt decrease of the surface pressure.

The same behavior was also found for the O–W interfaces stabilized with the protein species present in the supernatant, namely, expansion softening (or yielding) and compression hardening of the interfaces. As shown in Table 1, the O–W interfaces stabilized with the casein micelle

dispersion or supernatant also had similar elastic and viscous moduli at all amplitudes. However, the interfaces stabilized with the pellet redispersion displayed very weak responses at all amplitudes. No clear softening or hardening behavior was found for these interfaces. The plots are very narrow and show only a mild asymmetry at the highest amplitude. This type of response points either to an interface stabilized with surface active components that are irreversibly adsorbed and display only weak in-plane interactions between the molecules, or to a system in which diffusion between bulk and interface is very fast and (partially) compensates for changes in surface coverage induced by oscillation. The first harmonic based moduli of the O–W interfaces stabilized with the pellet redispersion were much lower than the ones of the interfaces stabilized with the casein micelle dispersion or supernatant (Table 1). Based on these observations, it appears that micellar caseins did not adsorb at the O–W interfaces, but small aggregates or monomers did.

In order to further distinguish whether the response of the O–W interfaces was dominated by small aggregates or monomers, dilatational oscillatory rheology was also applied on interfaces stabilized with

Table 1

First harmonic based elastic and viscous moduli (mN/m) of O–W or A–W interfaces stabilized with pellet redispersion, casein micelle dispersion, supernatant, or β -casein solution at different strains amplitudes. The frequency of the oscillation was 0.01 Hz.

O–W strain	pellet redispersion		casein micelle dispersion		supernatant		β -casein solution	
	E_1'	E_1''	E_1'	E_1''	E_1'	E_1''	E_1'	E_1''
0.1	1.78 ± 0.25	0.78 ± 0.05	19.21 ± 0.73	5.48 ± 0.41	14.62 ± 0.55	4.23 ± 0.12	1.69 ± 0.08	1.04 ± 0.02
0.15	2.09 ± 0.21	0.75 ± 0.01	15.38 ± 0.86	4.69 ± 0.27	13.55 ± 0.13	3.95 ± 0.18	1.67 ± 0.3	1.1 ± 0.01
0.2	2.31 ± 0.3	0.65 ± 0.01	12.88 ± 0.85	4.04 ± 0.24	12.19 ± 0.08	3.58 ± 0.14	1.8 ± 0.31	1.08 ± 0.06
0.3	2.66 ± 0.39	0.66 ± 0.04	9.41 ± 0.38	3.27 ± 0.18	9.26 ± 0.09	2.9 ± 0.15	1.75 ± 0.09	1.16 ± 0.01
A–W strain	pellet redispersion		casein micelle dispersion		supernatant		β -casein solution	
	E_1'	E_1''	E_1'	E_1''	E_1'	E_1''	E_1'	E_1''
0.1	10.32 ± 2.77	5.25 ± 2.59	12.76 ± 1.22	5.96 ± 2.81	29.74 ± 13.03	16.55 ± 8.45	33.67 ± 14.3	17 ± 4.45
0.15	10.24 ± 2.4	4.85 ± 2.51	13.27 ± 0.41	5.83 ± 2.54	27.38 ± 9.56	15.12 ± 7.09	34.12 ± 13.6	16.23 ± 4.03
0.2	10.04 ± 2.01	4.68 ± 2.26	14 ± 0.59	5.77 ± 2.23	26.14 ± 7.2	14.08 ± 6.18	35.47 ± 13.56	15.67 ± 3.3
0.3	9.87 ± 1.66	4.62 ± 2.03	14.65 ± 0.71	5.88 ± 1.96	25.97 ± 5.94	12.87 ± 5.1	39.25 ± 12.28	14.55 ± 1.83

β -casein. If monomers were responsible for the response, we would expect this protein to be dominant, in view of its surface activity. As shown in Fig. 3, compared to micellar casein dispersion and supernatant, β -casein stabilized O–W interfaces showed much weaker response during oscillation. β -casein has a highly hydrophilic head and a hydrophobic tail. Therefore, β -casein displays typical water soluble small molecular surfactant properties (Dickinson, 1998), which means that β -casein can adsorb at the interfaces quickly and spontaneously without forming a network. The in-plane interactions among these molecules are apparently relatively weak, since only low surface pressure values were found in Lissajous plots of O–W interfaces stabilized with β -casein, and the first harmonic based moduli were low (Table 1).

As micellar caseins were probably not adsorbing at the interfaces, and β -casein stabilized interfaces did not display a strong response during oscillation, the behavior of the O–W interfaces stabilized with casein micelle dispersions appeared to be dominated by small aggregates. Also, in view of the weak response of the redispersed pellet, a situation in which micelles did adsorb but subsequently fell apart seems unlikely.

3.3. Nonlinear interfacial rheology of A–W interfaces

Compared with O–W interfaces, A–W interfaces showed higher stiffness during oscillation, which was evidenced by the higher elastic moduli (Table 1). Similar findings were also reported by (Hinderink, Sagis, Schroën, & Berton-Carabin, 2020). The higher stiffness could be a result of the lower dielectric constant of air, as the dielectric constant of triglycerides is around 3, while the dielectric of air is around 1 (Benjamins, Lyklema, & Lucassen-Reynders, 2006). This will affect the balance between attractive and repulsive interactions among protein molecules at the A–W interface. A relative increase in attractive interactions could lead to stiffer interfaces.

A–W interfaces stabilized with either the casein micelle dispersion or the supernatant showed softening and hardening behaviors similar to those of O–W interfaces. A–W interfaces stabilized with the pellet redispersion displayed the mildest response during oscillation, which was evidenced by the flattest Lissajous plots and the smallest stiffness (Table 1). Therefore, it can be hypothesized that micellar caseins were not adsorbing at the A–W interfaces either.

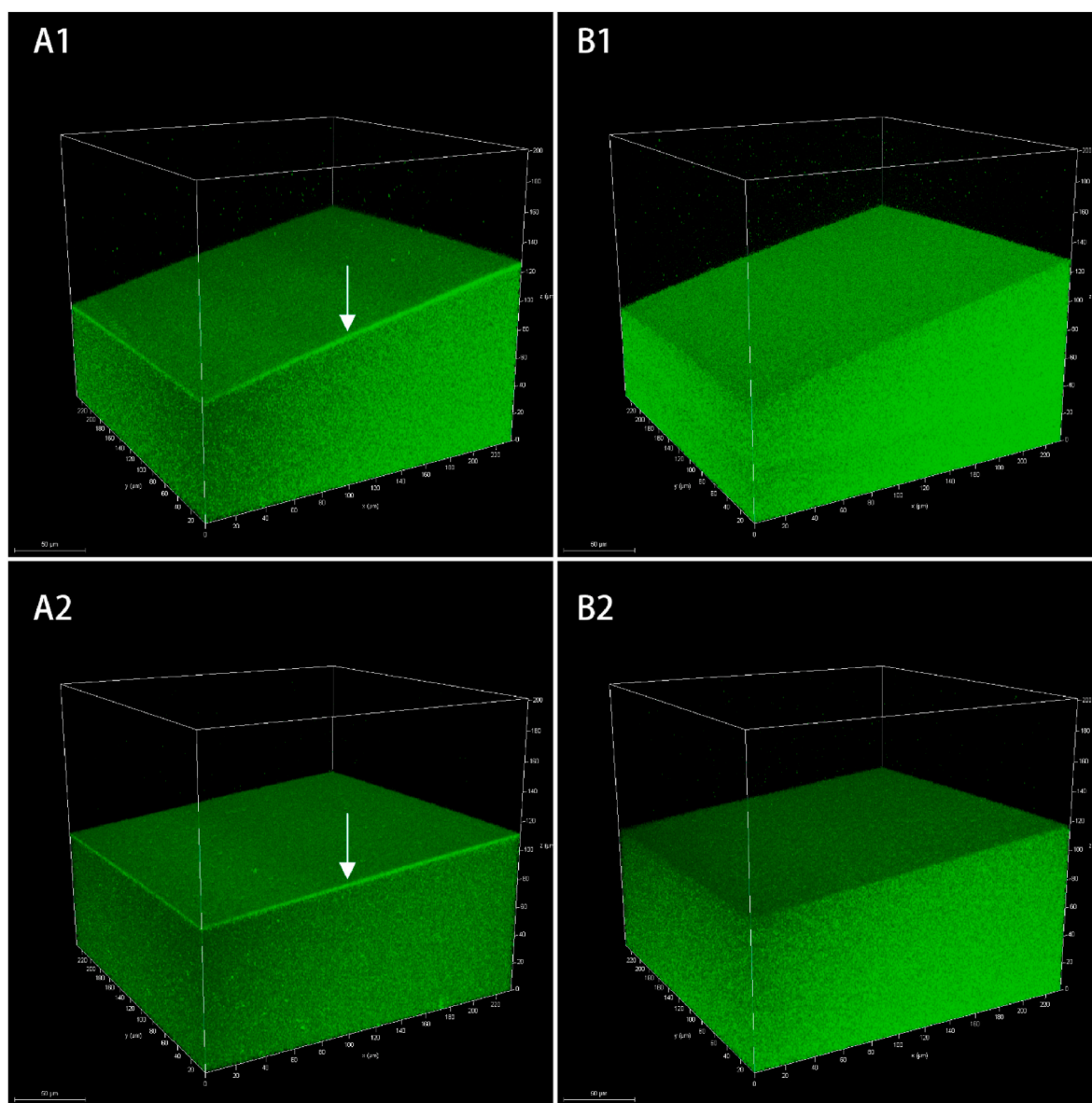


Fig. 4. Visualization of O–W (1) and A–W (2) interfaces stabilized with supernatant (A) or pellet redispersion (B). A 3-dimensional region (240*240*200 μm) was scanned by the MPM (see Fig. 1). The bottom part of each image is the water phase; the top part is the oil or air phase. The green color represents the proteins. The scale bar in the pictures represents 50 μm . (For interpretation of the references to color in this figure legend, the reader is referred to the Web version of this article.)

In order to estimate the role of individual casein fractions in the behavior of A-W interfaces, systems stabilized with β -casein were studied. As shown in Fig. 3, A-W interfaces stabilized with β -casein displayed softening and hardening similar to those observed for the casein micelle dispersion and supernatant. As the properties of interfaces stabilized with β -casein and the supernatant were similar, β -casein may be the dominant protein at the A-W interfaces. The differences among the response of pellet redispersion, casein micelle dispersion, supernatant, and β -casein solution were not as evident as in the case of the O-W interface. This may be because the amount of β -casein monomers in the samples were different. The pellet was re-dispersed in Milli-Q water, and micellar casein in the pellet may have partially fallen apart. Consequently, β -casein could be present also in the pellet redispersion.

3.4. Visualization of O-W and A-W interfaces

Based on the surface rheology results, it was hypothesized that micellar caseins do not adsorb at the O-W or the A-W interfaces, and that instead some smaller species such as small aggregates or monomers do. In order to confirm this hypothesis, O-W and A-W interfaces stabilized with pellet redispersion or supernatant were visualized by multiphoton microscopy (MPM) (Fig. 4). Distinct bright interfacial layers were observed for O-W and A-W interfaces stabilized with the supernatant (indicated by arrows). On the other hand, no distinct layers were found for interfaces stabilized with the pellet redispersion. The micelles remained in the bulk phase. The pictures clearly support the hypothesis that micellar caseins cannot adsorb at the O-W interface or the A-W interface. The protein species from the supernatant were more surface active and could accumulate at the interfaces. The pictures were in line with the rheology results. Further detailed characterizations of O-W and A-W interfaces were carried out by ellipsometry. The A-W interface was also further characterized by atomic force microscopy (AFM).

3.5. Thickness of O-W and A-W interfaces

The thickness of the studied A-W interfaces or O-W interfaces was characterized using ellipsometry. The thickness of the interfacial layer may also provide additional information on which species preferentially adsorb at the interface. The results are shown in Table 2. The pellet redispersion formed the thinnest O-W interface, with a thickness around 11 nm. The thickness values of O-W interfaces stabilized with the casein micelle dispersion or supernatant were comparable and were between 20 and 30 nm, which is in the range of the size of small aggregates. This is in line with the results of O-W interfacial rheology, where the dispersion and supernatant had similarly shaped Lissajous plots, and further supports the hypothesis that micellar caseins do not adsorb at the O-W interfaces, but those small aggregates do. The smaller size for the pellet redispersion may be due to adsorption of some residual subunits or monomers (~6 nm) present in that sample.

The thickness of A-W interfaces stabilized with pellet, micelle dispersion and supernatant was roughly the same, i.e. around 4.0 nm, which is close to the size of monomers (O'Connell, Grinberg, & de Kruijff, 2003). This also confirms the hypothesis that micellar caseins were not adsorbing on the A-W interfaces.

Table 2

Thickness of interfaces stabilized with casein micelles dispersion, pellet redispersion or supernatant, as measured by ellipsometry.

Interface	Pellet redispersion (nm)	Casein micelle dispersion (nm)	Supernatant (nm)
O-W	11.1 ± 1.5	22.2 ± 2.3	27.5 ± 0.1
A-W	4.2 ± 0.1	4.1 ± 0.1	4.4 ± 0.1

3.6. AFM imaging of A-W interfaces

The microstructure of A-W interfaces was further investigated by creating adsorption-based Langmuir-Blodgett (LB) films, which were analyzed with Atomic Force Microscopy (AFM). The surface pressure isotherms determined using a Langmuir trough are shown in Fig. 5. When the surface pressure increased to roughly 15 mN/m, the interfaces stabilized with the casein micelle dispersion, pellet redispersion, or supernatant all showed a change in slope, often associated with a phase transition from a liquid state to a solid state. The isotherm of the micelle dispersion mostly overlapped with the isotherm of the supernatant, which again suggests that the micelle dispersion and supernatant form a similar A-W interface in the liquid regime. To achieve the same surface pressure, the pellet stabilized interface needed to be compressed further, which may indicate a lower amount of material in the pellet redispersion which can adsorb at the interface.

The structure of the A-W interfaces was visualized at a surface pressure of 13 mN/m (Fig. 6 A1, B1, C1) and 23 mN/m (Fig. 6 A2, B2, C2), so just below and above the liquid-solid transition, respectively. At the lower surface pressure, the microstructures of all three interfaces were remarkably similar. This is in line with the result obtained with ellipsometry, and again indicates that micellar caseins did not adsorb at the A-W interfaces, but only monomers did. At the high surface pressure, all three samples formed dense interfacial films. The supernatant stabilized film formed the densest microstructure, and the pellet formed the least dense one. A lower density of the stabilizer could lead to weaker in-plane interactions among adsorbed proteins, which could contribute to the formation of weaker interfacial layers. The density differences among the samples might explain the A-W interfacial rheology results, where the moduli increased (pellet redispersion < casein micelle dispersion < supernatant, Table 1) with higher protein density at the A-W interfaces, as shown in the AFM images.

4. Conclusion

In this study we comprehensively investigated the role of the different fractions (micelles, small aggregates and casein fraction monomers) present in casein micelle dispersions at O-W and A-W interfaces. The results presented above clearly show that, although casein small aggregates and casein fraction monomers are the minor species in a casein micelle dispersion, they are the main surface-active components. Small aggregates and β -casein determine the mechanical

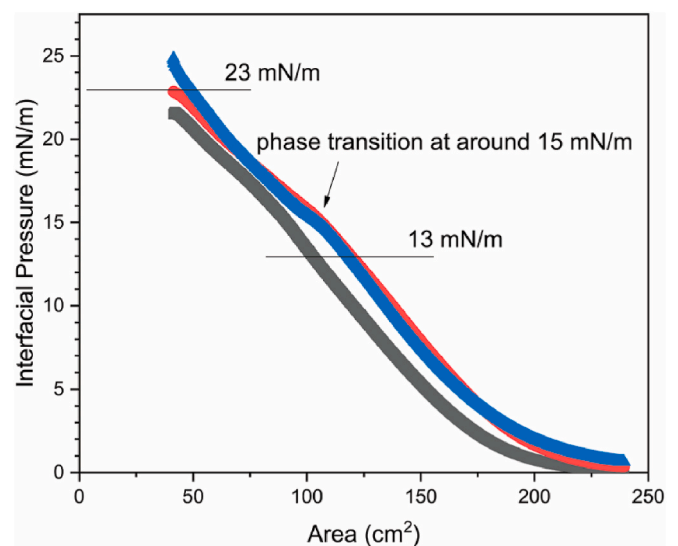


Fig. 5. Interfacial pressure isotherms of pellet redispersion (■), casein micelle dispersion (●) and supernatant (▲), obtained using a Langmuir trough.

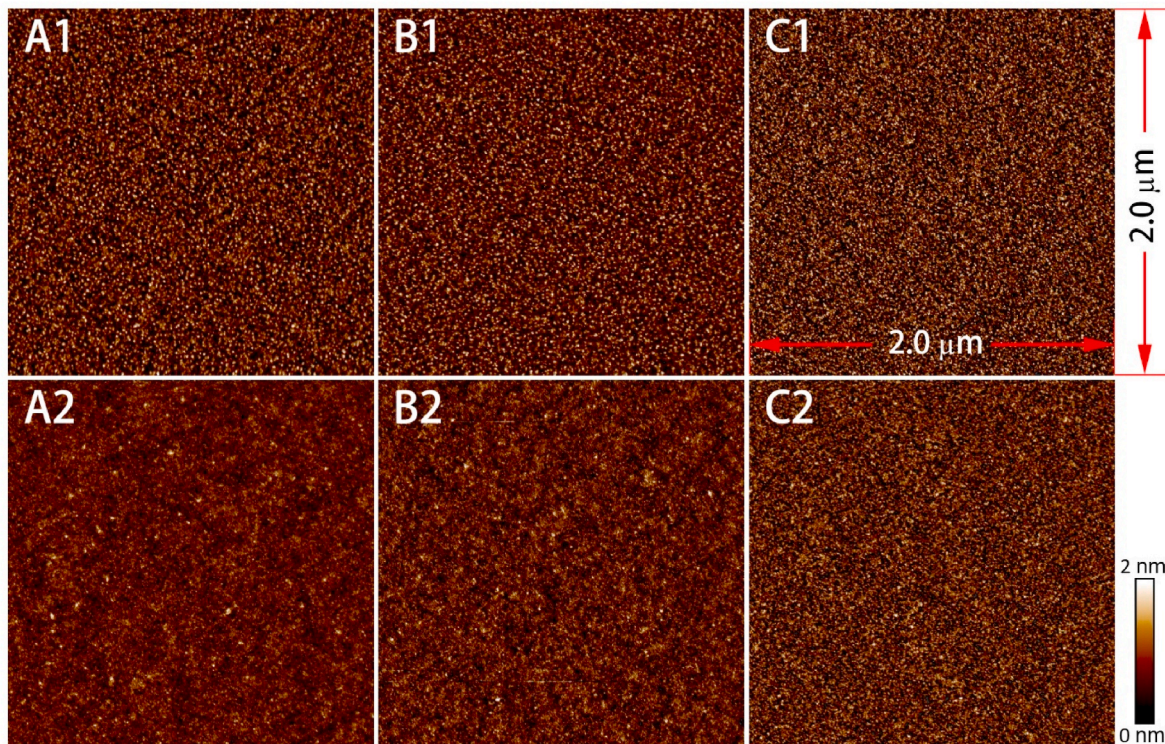


Fig. 6. AFM images of A-W interfaces stabilized with pellet redispersion (A), casein micelles dispersion (B) or supernatant (C). The surface pressure values during film sampling were 13 mN/m (1) and 23 mN/m (2). The area of each image represents $2.0 \times 2.0 \mu\text{m}^2$.

properties of O–W and A–W interfaces, respectively. Under the quiescent conditions applied in this study, we did not find any proof that casein micelles stabilize interfaces by a Pickering mechanism (Dickinson, 2015), as micelles cannot adsorb at O–W interfaces or A–W interfaces. A possible reason why the smaller species are dominant at the interface is their faster diffusion towards the interface, in view of their smaller size. There may also be differences in the magnitude of the adsorption barrier energy between micelles and smaller components.

A note we want to make here is that in our study the adsorption of the various fractions was diffusion based. In emulsion and foam preparation there is typically also a convective contribution to the transport of surface active components to the interface. This may be the reason that in some studies in electron microscopy pictures, micelles do appear to be at the oil-water or air-water interfaces (Anderson et al., 1987; Brooker, 1985; Jensen, 2013). However, their distribution on the surface tends to be sparse, and it is hard to distinguish whether they are actually adsorbed at the interface, or attached to a primary layer of molecules or smaller aggregates. Diffusion can still be a dominant factor in highly turbulent flows, because of the boundary layer that forms close to the bubble or oil droplet interface, in which the flow is laminar and parallel to the interface, and across which the motion of the surface active species towards the interface is mostly diffusive. But we cannot exclude the possibility that some micelles still do adsorb at/to the interface driven by convection.

We also studied only the initial state of the adsorption and did not perform long-term studies. Since emulsions tend to have long shelf lives, proteins may be displaced over time. If this were to happen the most likely scenario would be that the small aggregates are over time displaced by the casein monomer fraction, rather than by the micelles. Further measurements are needed to prove or disprove this scenario.

The approach we have outlined here, based on fractionation of a complex mixture, and on the study of the functionality of the individual fractions using a combination of (nonlinear) surface rheology and microstructural analysis (MPM, ellipsometry, AFM), can help in identifying the most relevant components in the mixture.

Author statement

Xilong Zhou: Investigation, Formal Analysis, Validation, Data Curation, Writing – Original Draft, Visualization.

Jack Yang: Investigation, Writing – Original Draft, Visualization.

Leonard M. C. Sagis: Conceptualization, Methodology, Writing - Review & Editing, Supervision, Project administration.

Guido Sala: Conceptualization, Methodology, Writing - Review & Editing, Supervision, Project administration.

Declaration of competing interest

The authors have declared that no competing interest exist. This manuscript has not been published and is not under consideration for publication in any other journal. All authors approve this manuscript and its submission to Food Hydrocolloids.

Acknowledgement

We acknowledge the funding from China Scholarship Council (CSC NO. 201706350123) for Xilong Zhou. We would like to thank Carljin Van Baalen (ETH) for providing the design of the special slide for interfacial visualization. We are also grateful for Arjen Bader's (WUR) technical support for the multiphoton excitation microscopy.

References

- Anderson, M., Brooker, B., & Needs, E. (1987). Stabilization/destabilization of dairy foams. In , Vol. 58. *Food emulsions and foams: Based on the proceedings of an international symposium organised by the food chemistry group of the royal society of chemistry at leeds from 24th-26th march 1986* (p. 100). Royal Society of Chemistry.
- Benjamins, J., Lyklema, J., & Lucassen-Reynders, E. H. (2006). Compression/expansion rheology of oil/water interfaces with adsorbed proteins. *Comparison with the air/water surface*, 22.
- Brooker, B. (1985). Observations on the air-serum interface of milk foams. *Food Structure*, 4(2), 12.

- Carr, A., & Golding, M. (2016). Functional milk proteins production and utilization: Casein-based ingredients. In P. L. H. McSweeney, & J. A. O'Mahony (Eds.), *Advanced dairy chemistry: Volume 1B: Proteins: Applied aspects* (pp. 35–66). New York, NY: Springer. New York.
- Chen, M., Bleeker, R., Sala, G., Meinders, M. B. J., van Valenberg, H. J. F., van Hooijdonk, A. C. M., et al. (2016). Particle size determines foam stability of casein micelle dispersions. *International Dairy Journal*, *56*, 151–158.
- Chen, M., Sala, G., Meinders, M. B. J., van Valenberg, H. J. F., van der Linden, E., & Sagis, L. M. C. (2017). Interfacial properties, thin film stability and foam stability of casein micelle dispersions. *Colloids and Surfaces B: Biointerfaces*, *149*, 56–63.
- Courthaudon, J. L., Girardet, J. M., Campagne, S., Rouhier, L. M., Campagna, S., Linden, G., et al. (1999). Surface active and emulsifying properties of casein micelles compared to those of sodium caseinate. *International Dairy Journal*, *9*(3–6), 411–412.
- Dalgleish, D. G., & Leaver, J. (1991). The possible conformations of milk proteins adsorbed on oil/water interfaces. *Journal of Colloid and Interface Science*, *141*(1), 288–294.
- Dalgleish, D. G., Spagnuolo, P. A., & Goff, D. H. (2004). A possible structure of the casein micelle based on high-resolution field-emission scanning electron microscopy. *International Dairy Journal*, *14*(12), 1025–1031.
- Dickinson, E. (1997). Properties of emulsions stabilized with milk proteins: Overview of some recent developments. *Journal of Dairy Science*, *80*(10), 2607–2619.
- Dickinson, E. (1998). Proteins at interfaces and in emulsions stability, rheology and interactions. *Journal of the Chemical Society, Faraday Transactions*, *94*(12), 1657–1669.
- Dickinson, E. (2001). Milk protein interfacial layers and the relationship to emulsion stability and rheology. *Colloids and Surfaces B: Biointerfaces*, *20*(3), 197–210.
- Dickinson, E. (2015). Microgels—an alternative colloidal ingredient for stabilization of food emulsions. *Trends in Food Science & Technology*, *43*(2), 178–188.
- Dickinson, E., & Matsumura, Y. (1994). Proteins at liquid interfaces: Role of the molten globule state. *Colloids and Surfaces B: Biointerfaces*, *3*(1), 1–17.
- Dombrowski, J., Dechau, J., & Kulozik, U. (2016). Multiscale approach to characterize bulk, surface and foaming behavior of casein micelles as a function of alkalisation. *Food Hydrocolloids*, *57*, 92–102.
- Dumpler, J. (2017). *Heat stability of concentrated milk systems: Kinetics of the dissociation and aggregation in high heated concentrated milk systems*. Springer.
- Ewert, J., Claassen, W., Gluck, C., Zeeb, B., Weiss, J., Hinrichs, J., et al. (2016). A non-invasive method for the characterisation of milk protein foams by image analysis. *International Dairy Journal*, *62*, 1–9.
- Fox, P. F., & McSweeney, P. L. (2013). *Advanced dairy chemistry* (Vol. 1). Parts A&B: Springer. Proteins.
- Hinderink, E. B. A., Sagis, L., Schroën, K., & Berton-Carabin, C. C. (2020). Behavior of plant-dairy protein blends at air-water and oil-water interfaces. *Colloids and Surfaces B: Biointerfaces*, *192*, 111015.
- Ho, T. M., Bhandari, B. R., & Bansal, N. (2021). Functionality of bovine milk proteins and other factors in foaming properties of milk: A review. *Critical Reviews in Food Science and Nutrition*, 1–21.
- Huppertz, T. (2010). Foaming properties of milk: A review of the influence of composition and processing. *International Journal of Dairy Technology*, *63*(4), 477–488.
- Jackson, R., & Pallansch, M. (1961). Influence of milk proteins on interfacial tension between butter oil and various aqueous phases. *Journal of Agricultural and Food Chemistry*, *9*(6), 424–427.
- Jensen, L. H. S. (2013). *Ultrastructure of emulsions - a comparative electron microscopy study*.
- Lazzaro, F., Saint-Jalmes, A., Violleau, F., Lopez, C., Gaucher-Delmas, M., Madec, M. N., et al. (2017). Gradual disaggregation of the casein micelle improves its emulsifying capacity and decreases the stability of dairy emulsions. *Food Hydrocolloids*, *63*, 189–200.
- Leman, J., Kinsella, J., & Kilara, A. (1989). Surface activity, film formation, and emulsifying properties of milk proteins. *Critical Reviews in Food Science and Nutrition*, *28*(2), 115–138.
- Liang, Y. C., Patel, H., Matia-Merino, L., Ye, A. Q., & Golding, M. (2013). Effect of pre- and post-heat treatments on the physicochemical, microstructural and rheological properties of milk protein concentrate-stabilised oil-in-water emulsions. *International Dairy Journal*, *32*(2), 184–191.
- Li, Y., Li, Y., Yuan, D. D., Wang, Y. N., Li, M. L., & Zhang, L. B. (2020). The effect of caseins on the stability and whipping properties of recombined dairy creams. *International Dairy Journal*, *105*.
- Mackie, A. R., Gunning, A. P., Ridout, M. J., Wilde, P. J., & Morris, V. J. (2001). Orogenic displacement in mixed β -Lactoglobulin/ β -Casein films at the air/water interface. *Langmuir*, *17*(21), 6593–6598.
- O'Connell, J. E., Grinberg, V. Y., & de Kruijff, C. G. (2003). Association behavior of β -casein. *Journal of Colloid and Interface Science*, *258*(1), 33–39.
- Qi, P. X. (2007). Studies of casein micelle structure: The past and the present. *Le Lait*, *87* (4–5), 363–383.
- Ridout, M. J., Mackie, A. R., & Wilde, P. J. (2004). Rheology of mixed β -Casein/ β -Lactoglobulin films at the Air–Water interface. *Journal of Agricultural and Food Chemistry*, *52*(12), 3930–3937.
- Roman, J. A., & Sgarbieri, V. C. (2006). The hydrophilic, foaming and emulsifying properties of casein concentrates produced by various methods. *International Journal of Food Science and Technology*, *41*(6), 609–617.
- Sagis, L. M., & Fischer, P. (2014). Nonlinear rheology of complex fluid–fluid interfaces. *Current Opinion in Colloid & Interface Science*, *19*(6), 520–529.
- San Martín-González, M. F., Roach, A., & Harte, F. (2009). Rheological properties of corn oil emulsions stabilized by commercial micellar casein and high pressure homogenization. *Lebensmittel-Wissenschaft und -Technologie- Food Science and Technology*, *42*(1), 307–311.
- Schiffer, S., Scheidler, E., Kiefer, T., & Kulozik, U. (2021). Effect of temperature, added calcium and pH on the equilibrium of caseins between micellar state and milk serum. *Foods*, *10*(4), 822.
- Scott, L. L., Duncan, S. E., Sumner, S. S., & Waterman, K. M. (2003). Physical properties of cream reformulated with fractionated milk fat and milk-derived components. *Journal of Dairy Science*, *86*(11), 3395–3404.
- Silva, N. F. N., Saint-Jalmes, A., de Carvalho, A. F., & Gaucheron, F. (2014). Development of casein microgels from cross-linking of casein micelles by genipin. *Langmuir*, *30* (34), 10167–10175.
- Tomas, A., Paquet, D., Courthaudon, J. L., & Lorient, D. (1994). Effect of fat and protein contents on droplet size and surface protein coverage in dairy emulsions. *Journal of Dairy Science*, *77*(2), 413–417.
- Walstra, P. (1990). On the stability of casein micelles. *Journal of Dairy Science*, *73*(8), 1965–1979.
- Walstra, P. (1999). Casein sub-micelles: Do they exist? *International Dairy Journal*, *9* (3–6), 189–192.
- Walstra, P., Wouters, J. T., & Geurts, T. J. (2005). *Dairy science and technology*. CRC press.
- Wu, S., Wang, G., Lu, Z., Li, Y., Zhou, X., Chen, L., et al. (2016). Effects of glycerol monostearate and Tween 80 on the physical properties and stability of recombined low-fat dairy cream. *Dairy Science & Technology*, *96*(3), 377–390.
- Yang, J., Thielen, I., Berton-Carabin, C. C., van der Linden, E., & Sagis, L. M. (2020). Nonlinear interfacial rheology and atomic force microscopy of air-water interfaces stabilized by whey protein beads and their constituents. *Food Hydrocolloids*, *101*, 105466.
- Zhang, Z., Dalgleish, D. G., & Goff, H. D. (2004). Effect of pH and ionic strength on competitive protein adsorption to air/water interfaces in aqueous foams made with mixed milk proteins. *Colloids and Surfaces B: Biointerfaces*, *34*(2), 113–121.
- Zhang, Z., & Goff, H. D. (2004). Protein distribution at air interfaces in dairy foams and ice cream as affected by casein dissociation and emulsifiers. *International Dairy Journal*, *14*(7), 647–657.
- Zhou, X., Chen, L., Han, J., Shi, M., Wang, Y., Zhang, L., et al. (2016). Stability and physical properties of recombined dairy cream: Effects of soybean lecithin. *International Journal of Food Properties*, *20*(10), 2223–2233.
- Zhou, X., Sala, G., & Sagis, L. M. (2020). Bulk and interfacial properties of milk fat emulsions stabilized by whey protein isolate and whey protein aggregates. *Food Hydrocolloids*, 106100.